International Journal of Thermophysics, Vol. 27, No. 2, March 2006 (© 2006)
DOI: 10.1007/s10765-006-0045-2

Thermophysical Properties of Solid Phase Hafnium at High Temperatures

N. D. Milošević[1,2] and K. D. Maglić[1]

Received August 19, 2005

The thermophysical properties of several hafnium samples with a content of zirconium below 1% were experimentally studied over a wide temperature range. The specific heat capacity and specific electrical resistivity were measured from 300 to 2340 K, the hemispherical total emissivity from 1000 to 2130 K, while the thermal diffusivity was measured in the range from 300 to 1470 K. The thermal conductivity and Lorentz number were computed from measured properties for the range from 300 to 1470 K. The specific heat capacity, specific electrical resistivity, and hemispherical total emissivity were measured by subsecond pulse calorimetry, and the thermal diffusivity using the laser flash method. Samples in the form of a thin rod or wire, and in the form of a thin disk were used in the first and second methods, respectively. For data reduction and computation of relevant parameters, recent literature values of the linear thermal expansion were used. The results are compared with literature data and discussed.

KEY WORDS: electrical resistivity; hafnium; heat capacity; hemispherical total emissivity; high temperatures; laser flash method; subsecond pulse calorimetry; thermal diffusivity.

1. INTRODUCTION

Hafnium belongs to the group of transition metals and, in nature, it is mostly present in zirconium minerals (1 to 5%). Hafnium is a supple shiny metal, easily treatable, but with a relatively high melting temperature (about 2504 K). Its properties are considerably influenced by the impurities of zirconium, and, in production, zirconium and hafnium are very difficult

[1] "Vinča" Institute of Nuclear Sciences, P.O. Box 522, 11001 Belgrade, Serbia and Montenegro.
[2] To whom correspondence should be addressed. E-mail: nenadm@vin.bg.ac.yu

to separate. Their chemistry is almost identical, but the density of hafnium is twice that of zirconium.

Hafnium has several remarkable properties such as a good absorption cross section for thermal neutrons (almost 600 times that of zirconium), and extremely high corrosion resistance. It is often used for reactor control rods, such as in nuclear submarines. Hafnium is successfully alloyed with iron, titanium, niobium, tantalum, and other metals, which makes it attractive for high temperature applications. Hafnium-based ceramics (carbides, borides, and nitrides) have extremely high melting temperatures and hardness, as well as high thermal and electrical conductivity and chemical stability; hafnium carbide is the most refractory binary composition known, with a melting point (m.p.) of 4163 K, and the nitride is the most refractory of all known metal nitrides with a m.p. of 3583 K. Hafnium is resistant to concentrated alkalis, but at elevated temperatures reacts with oxygen, nitrogen, carbon, boron, sulfur, and silicon. Being an efficient "getter" for oxygen and nitrogen, hafnium is used for gas-filled and incandescent lamps and vacuum tubes.

Accurate characterization of this element is, therefore, very important. In spite of that, there are few recent data of its thermophysical properties in the literature. Moreover, as zirconium is the most normal impurity (usually 3% of mass), there is a need for studying samples with low concentrations of this element. That is especially important for conductive properties, such as thermal diffusivity and specific electrical resistivity.

The first author who published results of Hf investigations was Zwikker [1] in 1926. By measuring the electrical resistivity, he observed the allotropic transformation of this metal in a large temperature region, however, with values underestimated in comparison to present ones, which were probably due to important impurity contents. Shortly after his study, DeBoer and Fast [2] mentioned that the presence of Zr might lower the phase transition temperature of pure Hf. Subsequently, a series of research was performed on the Hf transition temperature and some other properties and a relevant review of those studies until the 1960s was given by Bedford [3].

This paper presents experimental results for the thermophysical properties of several hafnium samples of a relatively high purity, ranging from about 99.0 to 99.6%. Using two transient state methods that have been standard for many years in this laboratory, various thermophysical properties were measured. The temperature range of the specific heat capacity, specific electrical resistivity, and hemispherical total emissivity measurements covers the structural hcp-bcc phase transition temperature (about 2000 K), where some significant changes in the material properties were detected.

2. EXPERIMENTAL SETTINGS

Two experimental methods were used: subsecond pulse calorimetry for specific heat capacity, specific electrical resistivity, and hemispherical total emissivity and the laser flash method for thermal diffusivity measurements. A general review of these techniques is given by Cezairliyan [4] and Taylor and Maglić [5], while some particular features regarding the applied data reduction can be found in Dobrosavljević and Maglić [6] and Milošević et al. [7].

2.1. Samples

Six different hafnium samples were provided: three were made from different hafnium wires and two from different hafnium block cylinders. The dimensions of the samples were measured by using two calibrated micrometers with the resolution of 10 and 20 μm, depending whether it was the wire diameter and the disk thickness or the wire length, respectively. The mass was measured with the resolution of 0.1 mg. The mean values and expanded uncertainties of physical parameters of each sample were obtained statistically, by averaging the values of repeated measurements, and they are given in Table I. The expanded uncertainties are given with a coverage factor of 2.

Before experiments were initiated, all samples were annealed for 1 hour in vacuum at 900 °C. Subsequent chemical analyses revealed the presence of impurities as given in Table II. After experiments were completed, the samples were not chemically analyzed.

The surface of sample 1 had an unexpected grayish color, which might have been attributed to carbon remaining from the wire drawing; so before chemical analysis, it was subjected to a treatment consisting of several heating cycles under high vacuum conditions, up to about 1100 K. As a result, its surface became brighter, but not as bright as the surface of the other samples. Subsequent chemical analysis showed that the carbon, whose overall concentration did not exceed 0.01%, was found mainly on

Table I. Physical Parameters of Hafnium Samples

Sample No.	Form	Length/Thickness (mm)	Diameter (mm)	Density ($kg \cdot m^{-3}$)
1	Wire	185.95 ± 0.02	2.410 ± 0.006	13189 ± 33
2	Wire	181.02 ± 0.02	3.977 ± 0.005	13222 ± 17
3	Wire	205.70 ± 0.02	0.937 ± 0.007	13157 ± 97
4	Disk	2.113 ± 0.008	9.402 ± 0.002	13239 ± 50
5	Disk	1.948 ± 0.007	9.920 ± 0.002	13225 ± 48

Table II. Chemical Compositions (in mass%) of Hafnium Samples

Sample No.	Purity (minimum)	Content of impurities
1	99.29	0.38 Zr, 0.01 C, 0.08 Ca, 0.065 Mo, 0.03 O, 0.023 Mg, 0.015 N, <0.01 Fe and Pb, <0.001 V
2	99.26	0.62 Zr, 0.056 Mo, 0.053 Ca, 0.008 Ni, 0.005 Fe, <0.001 V
3	98.99	0.98 Zr, 0.02 Mo, 0.006 Nb, 0.002 Fe, 0.001 Al and Si, <0.001 Ni, Ti, and Ca, 0.0008 Cu, <0.0001 Cr, Mg, and Mn
4	99.56	0.39 Zr, 0.02 Fe, 0.01 C, 0.005 N, 0.003 Al and Cu, <0.003 Ca and Mo, 0.002 Si, 0.001 Ti, <0.001 Mg, Nb, and Ni, 0.0004 Cr, <0.0001 Mn
5	99.41	0.55 Zr, 0.013 Ca and Fe, <0.005 Mo, 0.004 Y, <0.001 V

the sample surface, while the sample interior was practically free of this impurity. In order to preserve the sample diameter uniformity, it could not be exposed to polishing as a technique of carbon removal; thus, the sample was not altered. Consequently, for sample 1, higher values of emissivity were obtained compared with these from the literature.

The main impurity in all Hf samples was zirconium, with the mass concentrations ranging from 0.38 to 0.98%. In the first sample, traces of oxygen and nitrogen were found, and in the fourth, nitrogen. The lowest overall impurity concentration was for samples 4 and 5, as shown in Table II.

2.2. Measurement Description

2.2.1. Subsecond Pulse Calorimetry

General experimental procedure is described in detail in Ref. 6. In this research, W-Re 5% and W-Re 26% leads (50 μm in diameter) were used for temperature and voltage drop measurements. A thermocouple was welded intrinsically at the sample center, half-way between the power supply clamps. The intrinsic junction was used instead of the beaded one in order to reduce the finite response time of the thermocouple and to prevent possible perturbations at the point of temperature measurements. From the other side, two potential drop leads were welded at distances about 10 mm from the thermocouple, so the effective distance between them was always about 20 mm. After each time the potential leads were

fixed, this distance was established with repeated measurements using a traveling microscope and with an expanded uncertainty (coverage factor of 2) of about 10 μm.

The samples were held between two tungsten clamps in a vacuum chamber. The vacuum achieved by mechanical and oil diffusion pumps in series was usually between 4×10^{-3} and 9×10^{-3} Pa. One or two 12 V high-capacity batteries served as a dc source. For current measurements, a 1 mΩ standard resistor was used.

In total, three kinds of signals were measured simultaneously by a 16-bit multi-channel data acquisition system and by an accurate 24-bit digital multimeter (thermocouple emf measurements). With a 12 V dc source, the heating rate was about $600\,\mathrm{K \cdot s^{-1}}$, while with a 24 V dc source it was about $2300\,\mathrm{K \cdot s^{-1}}$. The initial temperature was always room temperature, and the maximum temperatures of the "effective" portion of the sample varied in different experiments, ranging from about 900 to 2450 K. In order to minimize the influence of the Thomson effect, the current direction was reversed in each run. The total number of runs for all samples (from 1 to 3) was 119.

As long as maximum temperatures were below 2200 K for samples 1 and 2, the experiments were reproducible, and without undesired effects, such as sample bending, etc. With an increase in temperature above 2200 K achieved by increasing pulse duration, an unexpected phenomenon occurred. The central portion of the sample, where the thermocouple was welded, suddenly became much brighter. When the maximum temperature was set for about 2450 K, each sample melted at the point where the thermocouple had been welded. An explanation was found for this phenomenon since hafnium and tungsten form a eutectic at about 2200 K (Fortov and Petukhov [8]). In fact, tungsten, from the welded thermocouple and voltage leads, and hafnium, from the sample, made an alloy with a surface brighter than that of the sample. Due to a significant reduction of the total emissivity for the thermocouple and voltage lead positions, the samples suffered overheating, which caused a rise of the heating rate. From that reason, with this combination of samples and materials for temperature and voltage measurements, results above 2200 K were not generally reliable due to the nonuniformity of the temperature distribution along the "effective" sample. Nevertheless, some temperature and voltage signals for temperatures up to 2340 K were feasible, which made possible application of the data reduction procedures and determination of the properties.

Due to the small diameter of sample 3 (less than 1 mm, see Table I), it could not tolerate extensive and prolonged heating as the first two samples did. The increase of the maximum temperature led to sample deterioration through bending and further thinning and resulted in premature melting.

For this reason, the maximum temperature of the last run (before melting) was only a few degrees below 2000 K, i.e., the phase transition was never reached with this sample. Moreover, a consequence of such conditions was that measurements of the specific heat capacity and specific electrical resistivity were less reliable, so those results were rejected and not presented in this work. On the other hand, the deterioration of sample 3 during the experiments did not influence significantly the determination of the hemispherical total emissivity. A decrease in the sample diameter at the thermocouple position was evaluated for each run, and accounted for in the final data reduction. Results were considered sufficiently reliable to be presented.

2.2.2. Laser Flash Method

In this method, the disk-shaped sample was placed in a specially designed graphite holder. In order to increase both thermal absorption and also thermal radiation of the sample, a thin layer ($< 10\,\mu$m) of a black colloidal carbon was deposited on the front and rear sample sides. The air pressure in the vacuum chamber was typically 0.3×10^{-3} Pa, which was achieved by mechanical and oil diffusion pumps in series.

The sample was heated to a desired temperature in a cylindrical tantalum foil furnace using a dc current. The sample reference temperature was measured with a thin "thermocoax" K-type thermocouple set next to the lateral side of the sample. A relation between the temperature detected by the thermocouple and the real sample temperature was established before thermal diffusivity measurements were initiated.

Temperature transients were obtained by energy pulses from a ruby laser, with a maximum output of 30 J and a typical pulse duration of 1 ms. For detection of temperature transients in the range from 300 to 470 K, a sensitive liquid nitrogen-cooled InSb infrared detector was used. In the range above 470 K, a water-cooled PbS IR photoresistor detector was applied. Signals from both detectors were measured with an accurate 24-bit digital multimeter.

The experiment consisted of 157 measurements, 77 for sample 4 and 80 for sample 5. The sample temperature was varied from ambient temperature up to 1485 K, with an average step of 50 K. Three signals were recorded at each reference temperature. The samples were inspected between each series of experiments, and no physical, including dimensional, changes of the sample were detected. Due to the laser beam interference with the colloidal carbon layer at the front sample side, this layer had to be renewed several times during the thermal diffusivity measurement series. The characteristic time of the transient temperature response was between 40 and 60 ms, while the average signal duration was about a factor of 8 larger.

2.3. Measurement Uncertainties

There were several sources of measurement uncertainties of the final properties: the errors of temperature measurements, the errors from measured quantities, such as sample dimensions, distance between the voltage leads, voltage drop over the effective sample, current through the sample, etc., the errors from computed quantities and functions, such as the sample temperature and the heating rate, and those caused by certain assumptions in the mathematical modeling of the related physical system, like the effect of a temperature gradient along and/or across the sample, etc.

In subsecond pulse calorimetry, which implies the use of thermocouples for temperature measurements, all sources of error in the final results are listed in Ref. 6. According to this reference, if one considers a number of experimental curves, the expanded uncertainties of the final specific heat capacity and specific electrical resistivity results were estimated to be 3 and 1%, respectively. Besides, by applying S-type thermocouples, the expanded uncertainty of temperature measurements was estimated to be a maximum of 5 K. In this research, however, due to the use of a W-Re thermocouple with somewhat lower sensitivity, the temperature measurements were estimated to have an expanded uncertainty of 5 K for temperatures up to 1300 K and an expanded uncertainty of 8 K for temperatures above 1300 K. Consequently, the expanded uncertainties of specific heat capacity and specific electrical resistivity became somewhat higher for temperatures above 1300 K.

Regarding the expanded uncertainty of the hemispherical total emissivity, it depends mainly on the error of temperature derivations and temperature measurements. By using repeated measurements, it was usually in the range from 3 to 8%, but could be significantly higher at temperatures below 1000 K.

In the laser flash method, the expanded uncertainty of the thermal diffusivity depends mostly on the error of sample thickness, which is usually less than 0.5%, and on the nonlinear heat-loss effects at high temperatures. By using a parameter estimation procedure (Milošević et al. [7]) and repeated mesurements, the expanded uncertainty of the thermal diffusivity was estimated to be in the range from 1 to 2%. Concerning the expanded uncertainty of temperature measurements, it was estimated to be a maximum of 2 K for the highest sample temperatures.

3. EXPERIMENTAL RESULTS AND DISCUSSION

For computing the thermophysical properties, the values of the linear thermal expansion coefficient were taken from Fortov and Petukhov [8].

These authors gave recommended values for polycrystalline hafnium with 0.66% Zr in the form of a quadratic polynomial,

$$\alpha_T = 6.578 \times 10^{-6} - 3.337 \times 10^{-10}(T - 293) + 5.754 \times 10^{-13}(T - 293)^2 \quad (1)$$

with an average expanded uncertainty of 2.3%. This equation is valid for temperatures up to 2000 K, i.e., to the phase transition point. In this work, however, because the error of the thermal expansion coefficient has a small influence on the uncertainty of the final results, Eq. (1) was also used for data reduction for the sample bcc phase.

3.1. Hemispherical Total Emissivity

For computing the specific heat capacity by subsecond calorimetry, it is necessary to know the temperature function of the hemispherical total emissivity of the investigated material. According to the procedure for obtaining this property, computed values of the hemispherical total emissivity are discrete, and very sensitive to errors introduced by fitting the function derivatives. As the phase transition takes place gradually, i.e., not instantly and uniformly along and across the sample, results for the hemispherical total emissivity within and in the vicinity of the phase transition region are not sufficiently reliable and accurate. Results obtained in this range, therefore, will not be presented in this work.

The values of the hemispherical total emissivity outside the phase transition region were obtained from experiments carried out on all three wire samples. At least 6 runs, all ending at approximately the same temperature (i.e., the temperature from which the sample cooling took place), were used to compute the average value of the hemispherical total emissivity at this temperature point.

Final results are shown in Fig. 1, together with available literature data. Their average values and their expanded uncertainties (coverage factor of 2) are given in Table III.

Results obtained for samples 2 and 3 below 2100 K, and the literature data of Zhorov [9], Peletskii and Druzhinin [10], Arutyunov et al. [11], Cezairliyan and McClure [12], and Paradis et al. [13] fall within a range confined between, roughly, 0.28 and 0.34, following a gentle, nearly linear increase. Results obtained for sample 1 lie much higher than all others, including the literature values, which are consistent with expectations based on the surface state discussed in Section 2.1. Since this sample had visible carbon impurity deposits on its surface, higher values of the hemispherical total emissivity were expected.

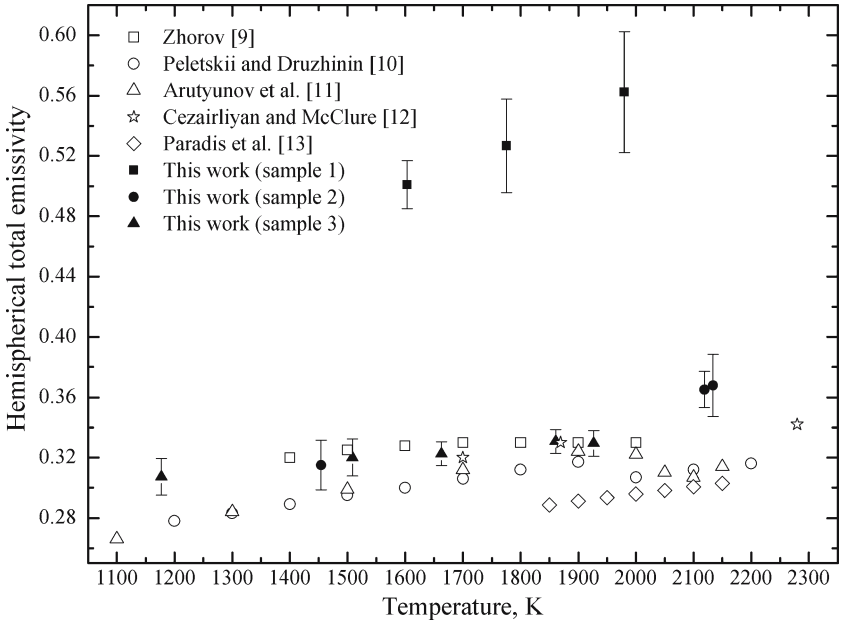

Fig. 1. Hemispherical total emissivity of hafnium.

Table III. Final Values and Expanded Uncertainties (Coverage Factor of 2) of the Hemispherical Total Emissivity of Hafnium

Sample 1			Sample 2			Sample 3		
T (K)	ε_{ht}	$U_{\varepsilon ht}$ (%)	T (K)	ε_{ht}	$U_{\varepsilon ht}$ (%)	T (K)	ε_{ht}	$U_{\varepsilon ht}$ (%)
935	0.459	7.0	1454	0.315	5.2	1177	0.307	3.9
1604	0.501	3.2	2119	0.365	3.3	1509	0.320	3.8
1776	0.527	5.9	2134	0.368	5.6	1663	0.323	2.5
1980	0.562	7.1				1861	0.331	2.4
						1927	0.329	2.6

[a]Not shown in Fig. 1.

An explanation for the data dispersion within the above boundaries could be found in the difference between the initial alloying impurities present in the samples, as well as due to the absorption of oxygen and nitrogen at their surfaces during sample heating. In spite of the fact that our experiments last only a very short time, this might have influenced to some extent two data points for sample 2 at about 2120 and 2134 K.

The results of various authors shown in Fig. 1 suggest that the hemispherical total emissivity of this metal slowly increases with temperature, following an almost linear relationship. Such functions were fitted for all our samples and used in later specific heat capacity calculations.

3.2. Specific Heat Capacity

According to the procedures described in Ref. 6, heat capacities as a function of temperature function were obtained from the measured voltage drop between potential leads, the electrical current through the sample, as well as from thermophysical and other parameters of the sample including its hemispherical total emissivity. Using the Kopp-Neumann rule, a correction for impurities was performed for zirconium and carbon (sample 1) and only zirconium for sample 2. Reference heat capacity data for zirconium and carbon were taken from Guillermet [14] and Touloukian and Buyco [15], respectively. Final results (measured and corrected for major impurities) with their expanded uncertainties (coverage factor of 2) for each sample are presented in Table IV.

All uncertainties were computed from data reduction procedures, where the influence of the error of each parameter was considered. For example, at high temperatures due to its large value and influence, the error of the hemispherical total emissivity plays the most important role. On the other hand, at low temperatures, large uncertainties are associated with the large scatter of measured data, which is typical for the experimental technique used here.

As one can see from Table IV, differences in impurities and composition do not significantly influence the measured heat capacity values (in the phase transition region, differences between the data were not assumed to be a strong function of the impurity concentration). The same applies to the sample geometry, although the diameters of the two samples differed by a factor of 2. For this reason, instead of discussing the results obtained for each single sample, analysis will be focused on the mean values of heat capacity, which are also presented in Table IV. They were computed from corrected values for each of the samples, and their uncertainties from the overall standard deviations that included standard deviations of the corresponding values from each sample. Therefore, the mean values and available literature data on the specific heat capacity of hafnium are presented in Fig. 2; values that correspond to temperatures from 1993 to 2021 K are not shown.

The maximum value of the specific heat capacity, which represents the minimum value of the first derivative of the transient temperature, was

Table IV. Final Values and Expanded Uncertainties (Coverage Factor of 2) of the Specific Heat Capacity of Hafnium

Sample 1				Sample 2			Mean values	
T (K)	c_p ($J \cdot kg^{-1} \cdot K^{-1}$) (measured values)	c_p ($J \cdot kg^{-1} \cdot K^{-1}$) (corrected values)	U_{cp} (%)	c_p ($J \cdot kg^{-1} \cdot K^{-1}$) (measured values)	c_p ($J \cdot kg^{-1} \cdot K^{-1}$) (corrected values)	U_{cp} (%)	c_p ($J \cdot kg^{-1} \cdot K^{-1}$) (from corrected values)	U_{cp} (%)
294	145.4	143.5	7.7	144.3	144.4	7.4	143.9	5.4
321	146.9	144.9	6.7	146.0	145.7	5.8	145.3	4.5
372	149.6	147.5	5.5	149.2	147.8	4.5	147.6	3.6
421	152.2	150.0	5.3	151.5	149.6	4.3	149.8	3.4
471	154.8	152.5	5.2	153.7	151.8	4.2	152.1	3.4
522	157.4	155.0	5.2	155.9	154.0	4.1	154.5	3.3
571	159.9	157.4	5.2	158.2	156.2	4.1	156.8	3.3
622	162.4	159.8	5.1	160.5	158.5	4.1	159.2	3.3
671	164.8	162.1	5.1	162.6	160.6	4.1	161.4	3.3
721	167.2	164.5	5.1	164.8	162.7	4.1	163.6	3.3
771	169.6	166.8	5.1	167.2	165.1	4.1	165.9	3.3
821	171.9	169.0	5.1	170.0	167.8	4.1	168.4	3.3
871	174.2	171.2	5.1	172.5	170.3	4.1	170.8	3.3
921	176.4	173.4	5.1	175.0	172.8	4.1	173.1	3.3
971	178.6	175.6	5.1	177.7	175.1	4.1	175.3	3.3
1021	180.8	177.7	5.1	180.2	177.6	4.1	177.6	3.3
1071	182.9	179.7	5.1	182.9	179.9	4.1	179.8	3.3
1121	185.0	181.8	5.1	185.4	182.0	4.1	181.9	3.3
1171	187.0	184.0	5.1	187.9	184.5	4.1	184.3	3.3
1221	189.0	186.0	5.1	190.3	186.8	4.1	186.4	3.3
1271	191.0	187.9	5.1	192.5	189.0	4.1	188.5	3.3
1321	192.9	189.8	5.1	194.6	191.2	4.1	190.5	3.3
1371	194.8	191.6	5.1	196.9	193.4	4.1	192.5	3.3

Table IV. *(Continued)*

Sample 1				Sample 2			Mean values	
T (K)	c_p ($J \cdot kg^{-1} \cdot K^{-1}$) (measured values)	c_p ($J \cdot kg^{-1} \cdot K^{-1}$) (corrected values)	U_{cp} (%)	c_p ($J \cdot kg^{-1} \cdot K^{-1}$) (measured values)	c_p ($J \cdot kg^{-1} \cdot K^{-1}$) (corrected values)	U_{cp} (%)	c_p ($J \cdot kg^{-1} \cdot K^{-1}$) (from corrected values)	U_{cp} (%)
1421	196.6	193.4	5.1	199.1	195.6	4.1	194.5	3.3
1471	198.4	195.2	5.1	201.1	197.5	4.1	196.4	3.3
1521	200.1	196.9	5.1	202.7	199.9	4.1	198.4	3.3
1571	201.8	198.6	5.1	204.4	202.0	4.1	200.3	3.3
1621	203.5	200.2	5.1	205.9	203.8	4.1	202.0	3.3
1671	205.1	201.8	5.1	207.4	205.6	4.1	203.7	3.3
1721	206.7	203.4	5.1	209.4	208.0	4.1	205.7	3.3
1771	208.3	204.9	5.1	210.8	210.0	4.1	207.5	3.3
1821	209.8	206.4	5.1	212.6	212.2	4.1	209.3	3.3
1871	211.2	207.8	5.1	214.9	214.5	4.1	211.2	3.3
1921	212.6	209.2	5.1	216.9	216.5	4.1	212.8	3.3
1971	214.0	210.6	5.1	227.5	225.2	10.8	217.9	6.1
1983	222.9	219.5	10.7	243.0	240.6	11.6	230.0	8.0
1993	271.0	267.5	12.9	293.6	291.2	14.0	279.4[a]	9.6
1998	389.5	386.0	18.6	396.2	393.8	18.8	389.9[a]	13.3
2004	1326.0	1322.5	63.4	961.5	959.2	45.4	1140.8[a]	41.5
2013	358.3	354.8	17.1	978.0	975.6	46.2	665.2[a]	34.2
2021	317.9	314.4	15.2	395.6	393.2	18.8	353.8[a]	12.5
2071	235.3	231.8	11.2	239.7	237.3	11.4	234.5	8.1
2121	194.8	191.2	5.1	194.6	192.1	4.1	191.7	3.3
2171	195.1	191.5	5.2	194.6	192.1	4.1	191.8	3.3
2222	195.4	191.8	5.2	194.7	192.1	4.1	191.9	3.4
2272	195.8	192.1	5.4				192.1	5.4
2321	196.5	192.8	5.4				192.8	5.4
2336	197.0	193.3	5.4				193.3	5.4

[a] Not shown in Fig. 2.

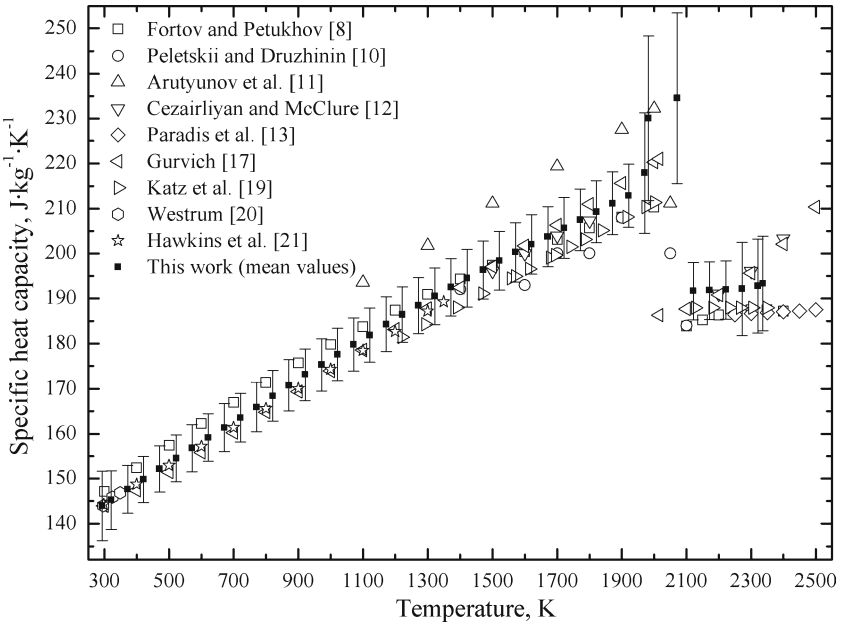

Fig. 2. Specific heat capacity of hafnium.

obtained by averaging at about 2004 K for sample 1, and at 2008 K for sample 2. As these points indicate the "middle" of the phase transition region, they can be considered as the most probable values of the phase transition temperature.

The expanded uncertainties of these temperatures (coverage factor of 2) were computed at the temperature corresponding to about a third of the maximum heat capacity value. These uncertainties were 9 and 4 K for samples 1 and 2, respectively, which were obtained statistically from numerous data curves and also considering the uncertainty of temperature measurements. Therefore, the final phase transition temperature could be taken as an average value of the above two temperatures as 2006 K, with a maximum expanded uncertainty of 5 K. In comparison to the value given by Touloukian and Buyco [16] (2023 ± 20 K), it is about 17 K less, but within the uncertainty. Cezairliyan and McClure [12] reported 2012 K, Fortov and Petukhov [8] reported 2015 K, Gurvich et al. [17] quoted 2016 K, while that of Binkele and Brunen [18] was highest, at 2050 K. Fortov and Petukhov [8] mentioned a large variation of this temperature, even 100 K for the case with a significant absorption of oxygen and nitrogen by the sample. However, DeBoer and Fast [2] noticed already in 1936 that the

presence of zirconium lowered the value of the phase transition point and that phenomenon was confirmed later by several authors.

Regarding heat capacity values, this research showed the appearance of a remarkable variation of the heat capacity around the phase transition point, i.e., within the phase transition region (Fig. 2). However, no other authors reported such behavior of this property around the phase transition point. Cezairliyan and McClure [12], who also used the subsecond calorimetry technique, did not report any values between 1850 and 2150 K, while Katz et al. [19] did the same from 2001 to 2127 K. Gurvich et al. [17] presented the data just up to, and above the phase transition point (2016 K), without mentioning the phase transition region. The reason for such differences between the present and literature data may be found in the nature of the dynamic method used, where one measures the variation of temperature as a function of time. As the structural phase transition takes place in a finite time period, temperature measurements, and thus the heat capacity values, are sensitive to that transformation.

In the hafnium hcp phase, up to the beginning of the phase transition region (at about 1975 K), the present values are generally in good agreement with literature results. At the lowest temperatures, the present results agree well with all literature data, especially with those given by Westrum and McClaine [20] (Hf 99.95 mass %) and Hawkins et al. [21]. At moderate temperatures, results from this research differ from those reported by Katz et al. [19] by about 3% (at 1320 K), but agree well with other data. More significant discrepancies appear at high temperatures, where the values of Arutyunov et al. [11] and Peletskii and Druzhinin [10] lie above and below, respectively, the present results, by about 7 and 4%, which exceeds the present estimated uncertainty limits. In the same temperature range our values agree very well with data published by Cezairliyan and McClure [12] and Gurvich et al. [17].

In the bcc phase, the present values lie about 2% above most other data, but within the estimated uncertainty limits. According to the data of Katz et al. [18], Paradis et al. [13], and Fortov and Petukhov [8], the specific heat capacity hardly varies with temperature in the bcc phase. Cezairliyan and McClure [12] and Gurvich et al. [17] indicated a more or less pronounced rise on approaching the melting point, which could be explained by the appearance of sample point defects at very high temperatures (Kraftmakher [22]).

3.3. Specific Electrical Resistivity

The values of the specific electrical resistivity of samples 1 and 2 were computed directly from the measured data of the voltage drop over the

Table V. Final Values and Expanded Uncertainties (Coverage Factor of 2) of the Specific Electrical Resistivity of Hafnium

Sample 1			Sample 2	
T (K)	ρ ($10^{-8}\Omega \cdot$m)	U_ρ (%)	ρ ($10^{-8}\Omega \cdot$m)	U_ρ (%)
293	46.1	3.4	38.6	2.6
323	50.1	3.2	42.8	2.4
373	58.1	2.8	49.5	2.2
423	64.0	2.6	56.2	2.0
473	71.0	2.5	63.0	1.8
523	78.2	2.3	69.7	1.7
573	85.3	2.2	76.4	1.6
623	92.2	2.0	82.9	1.5
673	99.0	2.0	89.5	1.4
723	105.6	1.9	95.7	1.4
773	112.1	1.8	101.9	1.3
823	118.4	1.7	107.9	1.3
873	124.4	1.7	113.7	1.2
923	130.1	1.7	119.7	1.2
973	135.4	1.6	125.1	1.1
1023	140.3	1.6	130.2	1.1
1073	145.3	1.6	134.9	1.1
1123	149.4	1.5	139.3	1.1
1173	153.3	1.5	143.3	1.1
1223	156.7	1.5	147.0	1.0
1273	160.0	1.5	150.1	1.0
1323	162.8	1.5	153.1	1.0
1373	165.1	1.4	155.8	1.0
1423	167.2	1.4	157.8	1.0
1473	168.8	1.4	159.7	1.0
1523	170.2	1.4	161.3	1.0
1573	171.5	1.4	162.5	1.0
1623	172.1	1.4	163.5	1.0
1673	173.0	1.4	164.5	1.0
1723	173.7	1.4	165.1	1.0
1773	173.9	1.4	165.7	1.0
1823	174.3	1.4	165.9	1.0
1873	174.5	1.4	166.3	1.0
1923	174.5	1.4	166.3	1.0
1973	174.5	1.4	166.3	1.0
1983	174.1	1.4	166.2	1.0
1993	173.8	1.4	166.0	1.0
1998	173.0	1.4	166.0	1.0
2003	171.9	1.4	165.4	1.0
2013	169.4	1.4	158.6	1.0
2023	168.3	1.4	157.3	1.0
2073	166.0	1.4	156.0	1.0

Table V. *(Continued)*

Sample 1			Sample 2	
2123	165.6	1.4	155.8	1.0
2173	164.6	1.5	155.8	1.0
2223	164.6	1.5	156.0	1.0
2273	164.8	1.5	156.5[a]	1.0
2323	165.5	1.4	157.2[a]	1.0
2336	165.9	1.4	157.4[a]	1.0

[a] Interpolated value.

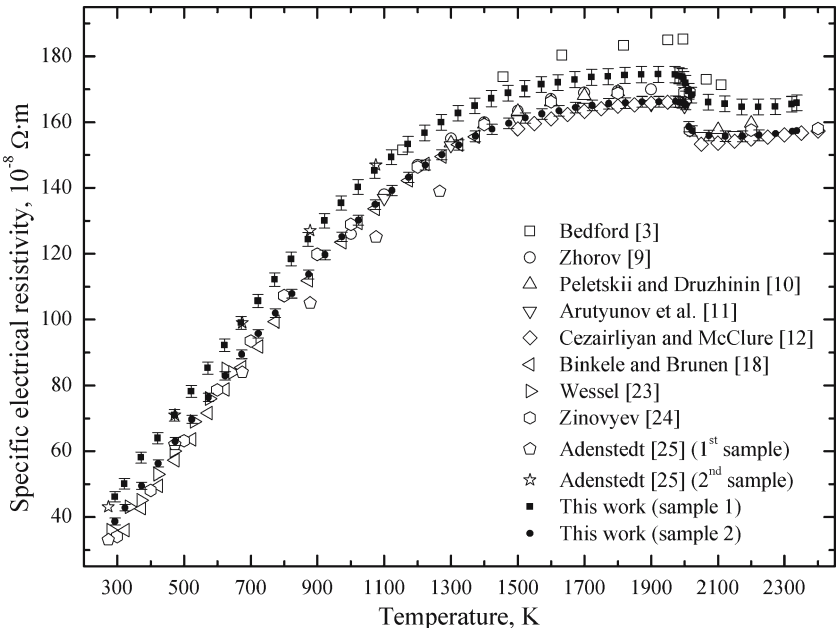

Fig. 3. Specific electrical resistivity of hafnium.

effective sample volume and the current through the sample, taking into account the thermal expansion of the sample. The final results were obtained by filtering raw data with a fast Fourier transformation. Final values are given in Table V and presented in Fig. 3 together with literature data.

In comparisons with literature data reported by Wessel [23], Zhorov [9], Peletskii and Druzhinin [10], Arutyunov et al. [11], Cezairliyan and McClure [12], Zinovyev [24], and Binkele and Brunen [18], results that correspond to sample 1 are higher from about 30% at room temperature

to 5.8% at 1373 K. The data of Adenstedt [25] for their first sample fall below the rest from about 700 K. However, his results for the second sample virtually coincide with our values. The main difference between two hafnium samples tested by Adenstedt [25] was in the content of the impurities: while the first sample did not include oxygen at all, another one had about 0.037 mass% of this element. Other impurities in Adenstedt's samples had similar concentrations, including those of Zr (between 0.7 and 0.8 mass%). The highest data in the high temperature region were published by Bedford [3]. He reported impurities of 2.4 mass% of Zr, 0.032 of mass% of oxygen, and 0.01 mass% of nitrogen in his hafnium sample. In addition, his values showed a systematic increase of the electrical resistivity with the number of experiments, probably indicating further sample oxidation. Binkele and Brunen [18] used a sample with 1.2 mass% of Zr, and their results match well those from Zinovyev [24] and Cezairliyan and McClure [12] who used samples with 3 mass% of Zr. Considering the above, it may be that the zirconium impurity does not influence the electrical resistivity as much as do other impurities, e.g., oxygen. Present results could confirm this statement, because, while no traces of oxygen or other gaseous elements, such as N and H were detected in sample 2 (see Table II), 0.03 mass% of oxygen was found in sample 1 and, probably, the content of this element increased during the experiments. In addition, the presence of carbon in sample 1 could further contribute to the increase of its specific electrical resistivity.

The specific electrical resistivity results for sample 2 are in more or less good agreement with other literature data as shown in Fig. 3. At the lowest temperatures, the present values agree very well with those from Wessel [23], but are about 13% higher than values from Zinovyev [24]. As the temperature increases, the agreement between the present and literature data becomes better; thus, in the middle temperature range from about 800 to 1500 K, the present values agree well with data from Refs. 9-11, 18, and 24. From 1500 K to the transition point, current results agree best with these of Arutyunov et al. [11] and Cezairliyan and McClure [12]. Above the transition point, the present data agree also with those of Zinovyev [24]. The values of Adenstedt [25] (first sample) lie about 8% below all other data in the middle temperature range, however, no obvious reason is known for this behavior.

If one considers the uncertainty limits of published data (not reported in some papers), the overall agreement between the present results obtained for sample 2 and most other literature values is good. It should be added that, except for this work and that of Zinovyev [24], no other experimental studies of the electrical resistivity of solid hafnium over such a wide temperature range is found in the literature.

3.4. Thermal Diffusivity

Hafnium samples 4 and 5 in the form of thin disks, and with impurity contents given in Table II, were used for the thermal diffusivity measurements. Experimental data, obtained by the laser flash method were analyzed by the parameter estimation procedure. Correction of the sample thickness due to the linear thermal expansion was carried out according to Eq. (1). Final results for both samples, mean values, and their expanded uncertainties (coverage factor 2) are given in Table VI. Mean values are presented in Fig. 4, along with literature data.

As one can see in Table VI, thermal diffusivity values of the two samples agree in the temperature region from room temperature up to about

Table VI. Final Values and Expanded Uncertainties (Coverage Factor of 2) of the Thermal Diffusivity of Hafnium

Sample 4			Sample 5			Mean values		
T (K)	a ($10^{-6}\,m^2 \cdot s^{-1}$)	U_a (%)	T (K)	a ($10^{-6}\,m^2 \cdot s^{-1}$)	U_a (%)	T (K)	a ($10^{-6}\,m^2 \cdot s^{-1}$)	U_a (%)
293	13.81	1.0	285	13.63	1.9	289	13.72	1.1
326	13.15	1.0	321	13.19	1.1	324	13.17	0.8
375	12.45	0.3	386	12.17	1.1	381	12.31	0.6
423	11.85	0.5	433	11.74	2.3	428	11.80	1.2
459	11.49	0.8	492	11.18	2.1	475	11.34	1.1
521	10.81	2.8	530	10.84	0.6	525	10.82	1.4
568	10.47	1.4	579	10.57	1.3	574	10.52	0.9
615	10.24	1.4	618	10.40	0.9	617	10.32	0.8
664	10.03	0.9	664	10.17	2.8	664	10.10	1.5
714	9.91	0.7	715	9.92	1.6	714	9.91	0.9
767	9.72	0.4	760	9.79	1.8	764	9.76	0.9
817	9.57	0.3	825	9.67	1.6	821	9.62	0.8
862	9.46	0.3	874	9.59	0.8	868	9.53	0.4
914	9.36	1.5	919	9.54	1.6	917	9.45	1.1
962	9.32	0.2	965	9.54	0.9	964	9.43	0.5
1012	9.29	0.4	1017	9.54	1.7	1015	9.41	0.9
1065	9.26	0.3	1065	9.53	1.5	1065	9.40	0.8
1113	9.27	0.1	1118	9.59	1.6	1115	9.43	0.8
1162	9.40	2.1	1174	9.60	1.2	1168	9.50	1.2
1215	9.45	1.0	1222	9.65	1.0	1219	9.55	0.7
1262	9.43	3.4	1277	9.81	1.9	1269	9.62	1.9
1314	9.50	1.5	1332	9.85	1.6	1323	9.67	1.1
1362	9.70	1.6	1370	10.01	1.8	1366	9.85	1.2
1417	9.96	2.8	1430	10.21	1.5	1424	10.08	1.6
1463	10.02	1.9	1472	10.54	1.9	1468	10.28	1.3

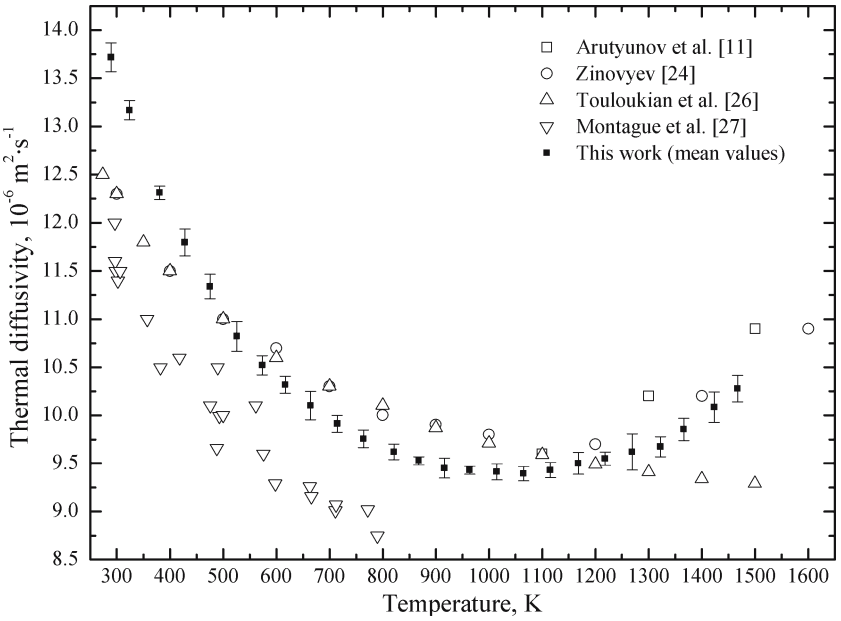

Fig. 4. Thermal diffusivity of hafnium.

900 K. Above that temperature, however, differences become more significant. At high temperatures, the thermal diffusivity of sample 5 is greater than that of sample 4 and this difference reaches 5% at about 1465 K. The reasons for such a discrepancy could lie either in the impurity level (according to Table II, sample 4 had some nitrogen and carbon impurities), or in the possible oxidation of sample surfaces during the experiments at high temperatures.

Only four sets of relevant data on the thermal diffusivity of hafnium were found in the literature: three of them were experimentally measured and one was provisional. Touloukian et al. [26] gave a theoretical estimation of the thermal diffusivity for pure hafnium, with 15% uncertainty below 900 K and 25% uncertainty above this temperature. According to this prediction (see Fig. 4), the thermal diffusivity follows an exponential fall in the temperature range of consideration. On the experimental side, Montague et al. [27] tested several hafnium samples in the range from 300 to 800 K (with no impurity information). Their data started just below the provisional values, and were about 10% lower at 750 K, when they experienced formation of an oxide layer on the sample surface, which limited their measurement range. On the other hand, Arutyunov et al. [11]

measured the thermal diffusivity of hafnium (with 0.65 mass% of Zr) only at high temperatures, from 1100 to 2050 K, while Zinovyev [24] measured this property over a large temperature range, from ambient temperature to the melting point. For the sake of comparisons, only data up to 1600 K are presented in Fig. 4.

In contrast to the estimated values of Touloukian et al. [26], Arutyunov et al. [11] reported a rise of thermal diffusivity values from 1100 K, and the same behavior was detected by Zinovyev [24]. The data from the latter are in excellent agreement up to 1000 K with those from Touloukian et al. [26], but diverge from them at higher temperatures. Our results follow the same trend as those of Zinovyev [24]. The thermal diffusivity decreases above the ambient temperature, and at 1065 K, is about one third of its room temperature value. After that point, the thermal diffusivity gradually increases. The maximum difference between the present results and those of Zinovyev [24] is at ambient temperature, where the difference is about 7%, decreasing to about 1% at 1100 K.

3.5. Thermal Conductivity and Lorentz Number

These two properties were computed by using the above experimentally measured values. The thermal conductivity was computed from the simple relation $k = \rho_v c_p a$, where ρ_v is the density of the sample, while the Lorentz number was calculated from the ratio $L = k\rho/T$. Corresponding mean values were taken for c_p, a, and ρ_v ($13219 \pm 20\,\mathrm{kg \cdot m^{-3}}$ at ambient temperature), while data obtained from sample 2 were considered for ρ. Corrections for the linear thermal expansion were applied to the mean values of ρ_v, using Eq. (1) for the thermal expansion coefficient.

The computed thermal conductivities of hafnium are presented in Fig. 5, together with available literature data. The maximum expanded uncertainties (coverage factor of 2) range from 5.5% (at 289 K) to 3.4% (at 868 K). It can be seen that in the temperature range of investigation the values from the current study are generally in good agreement with previous results. As the uncertainty of the computed thermal conductivity depends strongly on the uncertainty of the measured heat capacity and thermal diffusivity, this could indicate accurate and reliable measurements of the latter two properties.

While the recommended values of the thermal conductivity of Touloukian et al. [28] suggested small variations of the thermal conductivity before and after the minimum at about 900 K, Binkele and Brunen [18] reported a significant variation of this property both before and after this temperature and Zinovyev [24] showed a significant increase above this temperature. Timrot et al. [29] and Arutyunov et al. [11] measured

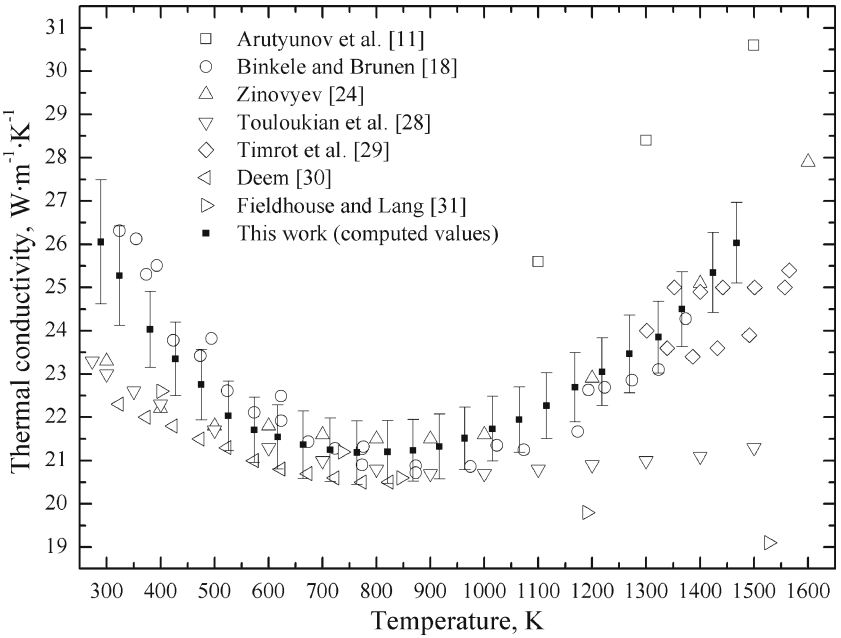

Fig. 5. Thermal conductivity of hafnium.

the thermal conductivity only at high temperatures, while Deem [30] performed measurements only in the region up to 820 K. In the corresponding temperature range, values from Arutyunov et al. [11] are higher than all other data by about 20%. Fieldhouse and Lang [31] were the only authors who reported a decrease of the thermal conductivity in the entire range from ambient to 1530 K.

The results from this work agree well with the data of Binkele and Brunen [18] and Zinovyev [24] over the entire temperature range. As Binkele and Brunen [18] used samples with 1.2 mass% Zr, Deem [30] with 2 mass% Zr, Fieldhouse and Lang [31] with 1 mass% Zr, and Arutyunov et al. [11] with 0.65 mass% Zr, it can be concluded that a small amount of the Zr impurity does not influence significantly the thermal conductivity, so the differences between data sets are probably a consequence of different experimental methods, data reduction procedures, and/or sample preparation.

For the Lorentz number, computed values and available literature data are presented in Fig. 6. At the lowest temperatures, the present results are much higher than the theoretical value for metals ($2.45 \times 10^{-8}\,\mathrm{W}\cdot\Omega\cdot\mathrm{K}^{-2}$), but this difference decreases with temperature. In the region from about 800 to 1400 K the Lorentz number has an approxi-

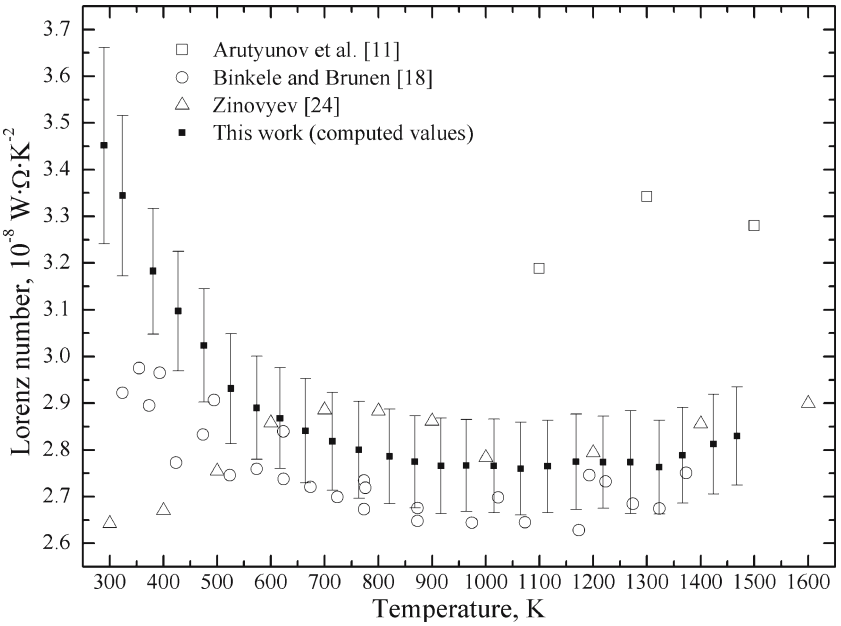

Fig. 6. Lorentz number for hafnium.

mately constant value of about $2.8 \times 10^{-8}\,\mathrm{W \cdot \Omega \cdot K^{-2}}$. Similar values in the temperature region of consideration were observed by Zinovyev [24] and Binkele and Brunen [18]. At the highest temperatures, the Lorentz number of Arutyunov et al. [11] differs considerably from all other data, which is a consequence of discrepancies between corresponding thermal conductivity values.

According to the present results, the influence of electronic scattering due to the imperfections of the sample structure (especially in the first two samples, which consisted of many impurities, such as C, Ca, Mo, and gaseous elements) decreases with temperature.

4. CONCLUSIONS

In this study five different samples whose purity varied from 99.0 to 99.6 mass% were used for determination of the properties of hafnium. Based on this work, the following conclusions could be stated.

- In the range from 1150 to 2150 K, the hemispherical total emissivity of hafnium lies between 0.30 and 0.38, with a virtually linear increase with temperature.

- The presence of carbon impurity on the surface of one hafnium sample resulted in a significantly higher emissivity, while no obvious effect of different zirconium content on that parameter was detected.
- The specific heat capacity, specific electrical resistivity, phase transition temperature, and thermal diffusivity of hafnium in the temperature range of consideration are generally in good agreement with the majority of previous available literature data.
- The specific heat capacity varies abruptly around the phase transition point, in a way typical of the applied experimental method.
- The specific electrical resistivity of hafnium seems to depend more on nonmetallic and gaseous impurities than on metallic ones, e.g., on the zirconium impurity.
- The thermal diffusivity of hafnium shows a parabolic behavior in the temperature range from 300 to 1470 K.
- The computed thermal conductivity and Lorentz number of hafnium in the temperature range of consideration agree, in general, with literature data, which may indicate the accuracy and reliability of the experimental methods and procedures applied in measuring the above properties.

Measurements of the thermal diffusivity at temperatures above 1500 K, and in the region of the phase transition point will be the subject of future research.

REFERENCES

1. C. Zwikker, *Physica* **6**:361 (1926).
2. J. H. DeBoer and J. D. Fast, *Rec. Trav. Chim*. **55**:456 (1936).
3. R. G. Bedford, *J. Appl. Phys*. **36**:113 (1965).
4. A. Cezairliyan, in *Compendium of Thermophysical Property Measurement Methods, Vol. 1 - Survey of Measurement Techniques*, K. D. Maglić, A. Cezairliyan, and V. E. Peletsky, eds. (Plenum, New York, 1992), pp. 643–668.
5. R. E. Taylor and K. D. Maglić, in *Compendium of Thermophysical Property Measurement Methods, Vol. 1 - Survey of Measurement Techniques*, K. D. Maglić, A. Cezairliyan, and V. E. Peletsky, eds. (Plenum, New York, 1992), pp. 305–336.
6. A. S. Dobrosavljević and K. D. Maglić, *High Temp. High Press*. **21**:411 (1989).
7. N. D. Milošević, M. Raynaud, M. Laurent, and K. D. Maglić, *Thermal Sci*. **3**:71 (1999).
8. V. E. Fortov and V. A. Petukhov, presented at IAEA Meeting, Vienna, Austria, July 16–19, 2001.
9. G. A. Zhorov, *High Temp*. **8**:501 (1970).
10. V. E. Peletskii and V. P. Druzhinin, *High Temp*. **9**:490 (1971).

11. A. V. Arutyunov, S. N. Banchila, and L. P. Filippov, *High Temp*. **10**:375 (1972).
12. A. Cezairliyan and J. L. McClure, *J. Res. Natl. Bur. Stand.* (*U.S.*) **79A**:431 (1975).
13. P.-F. Paradis, T. Ishikawa, and S. Yoda, *Int. J. Thermophys*. **24**:239 (2003).
14. A. F. Guillermet, *High Temp. High Press*. **19**:119 (1987).
15. Y. S. Touloukian and E. H. Buyco, *Thermophysical Properties of Matter, Vol. 5: Specific Heat of Nonmetallic Solids*, Y. S. Touloukian and C. Y. Ho, eds. (IFI/Plenum, New York, Washington, 1970), p. 9.
16. Y. S. Touloukian and E. H. Buyco, *Thermophysical Properties of Matter, Vol. 4: Specific Heat of Metallic Elements and Alloys*, Y. S. Touloukian and C. Y. Ho, eds. (IFI/Plenum, New York, Washington, 1970), p. 87.
17. L. V. Gurvich, *Thermodynamical Properties of Elements and Compounds*, L. V. Gurvich, I. V. Veitz, V. A. Medvedev, G. A. Bergman, V. S. Yungman, G. A. Hachkuruzov, V. S. Yurishtz, O. V. Dorofeyeva, E. L. Osina, P. I. Tolmach, I. N. Przevalskii, I. N. Nazarenko, N. M. Aristova, E. A. Shenyavskaya, L. N. Gorohov, A. L. Rogatzkii, M. E. Efimov, V. Ya. Leonidov, Yu. G. Havt, A. G. Efimova, S. E. Tomberg, A. V. Gusarov, N. E. Handamirova, G. N. Yurkov, L. R. Fokin, L. F. Kuratova, and V. G. Ryabova, eds. (Nauka, Moscow, 1982), p. 450. [in Russian]
18. L. Binkele and M. Brunen, *Thermal Conductivity, Electrical Resistivity and Lorentz Function Data for Metallic Elements in the Range 273 to 1500 K* (KFA Forschungszentrum Jülich GmbH, 1994), p. 63.
19. S. A. Katz, V. Ya. Chekhovskoi, and M. D. Kovalenko, *Teplofiz. Visok. Temper*. **23**:395 (1985). [in Russian]
20. E. F. Westrum Jr., *ASD TDR 62–204*, L.A. McClaine, ed., Pt. 3, 189 (1964).
21. D. T. Hawkins, M. Onillon, and R. L. Orr, *J. Chem. Eng. Data* **8**:628 (1963).
22. Y. Kraftmakher, *Equilibrium Point Defects and Thermophysical Properties of Metals* (World Scientific Publishing, Singapore, 2000), p. 102.
23. E. T. Wessel, *USAEC Publ. AECU-3693* (1956), pp. 1–46.
24. V. E. Zinovyev, *Metallurgia* (Nauka, Moscow, 1989), p. 384. [in Russian]
25. H. K. Adenstedt, *Am. Soc. Metals Preprint* 1W:19 (1951).
26. Y. S. Touloukian, R. W. Powell, C. Y. Ho, and M. C. Nicolaou, *Thermophysical Properties of Matter, Vol. 10: Thermal Diffusivity*, Y. S. Touloukian and C. Y. Ho, eds. (IFI/Plenum, New York, Washington, 1973), p. 77.
27. S. A. Montague, C. W. Draper, and G. M. Rosenblatt, *J. Phys. Chem. Solids* **40**:987 (1979).
28. Y. S. Touloukian, R. W. Powell, C. Y. Ho, and P. G. Klemens, *Thermophysical Properties of Matter, Vol. 1: Thermal Conductivity*, Y. S. Touloukian and C. Y. Ho, eds. (IFI/Plenum, New York, Washington, 1970), p. 138.
29. D. L. Timrot, V. E. Peletskii, and V. Yu. Voskresenskii, *High Temp.* **4**:808 (1966).
30. H. W. Deem, *USAEC Rept. BMI-853* (1953).
31. I. B. Fieldhouse and J. I. Lang, *WADD-TR-60–904* (Armour Res. Foundation, 1961).